

# Scavenging Phenomenon Elucidated from $^{234}\text{Th}/^{238}\text{U}$ Disequilibrium in Surface Water of the Taiwan Strait

Ching-Ling Wei<sup>1,\*</sup>, Jing-Ru Tsai<sup>1</sup>, Yen-Ruei Hou<sup>1</sup>, Liang-Saw Wen<sup>1</sup>,  
David D. Sheu<sup>2</sup>, and Wen-Chen Chou<sup>3</sup>

<sup>1</sup>*Institute of Oceanography, National Taiwan University, Taipei, Taiwan, ROC*

<sup>2</sup>*Institute of Marine Geology and Chemistry, National Sun Yat-sen University, Kaohsiung, Taiwan, ROC*

<sup>3</sup>*Institute of Marine Environmental Chemistry and Ecology, National Taiwan Ocean University, Keelung, Taiwan, ROC*

Received 1 April 2009, accepted 26 August 2009

---

## ABSTRACT

Concentrations of dissolved ( $^{234}\text{Th}_d$ ) and particulate ( $^{234}\text{Th}_p$ )  $^{234}\text{Th}$  in surface water at 38 stations in the Taiwan Strait were determined for samples collected in May 2006. The spatial distribution of  $^{234}\text{Th}$  in the Taiwan Strait is controlled by advective input of Kuroshio Branch Water via the Peng-Hu Channel and fast removal due to the high input of riverine particulates from the Cho-Sui River. A scavenging model involving physical transport was applied to the  $^{234}\text{Th}_d$  and  $^{234}\text{Th}_p$  data to estimate scavenging and removal rates of  $^{234}\text{Th}$ . Estimated scavenging rate ranges from 32 to 703  $\text{dpm m}^{-3} \text{d}^{-1}$  and the removal rate ranges from 24 to 560  $\text{dpm m}^{-3} \text{d}^{-1}$ . Using  $^{234}\text{Th}$  as a proxy of particulate organic carbon, we estimate that the removal rate of POC from surface water of the Taiwan Strait ranges from  $0.3 \pm 1.5 \text{ mmol-C m}^{-3} \text{d}^{-1}$  off southwestern Taiwan to  $10.2 \pm 3.5 \text{ mmol-C m}^{-3} \text{d}^{-1}$  in the central Taiwan Strait.

Key words:  $^{234}\text{Th}$ , Taiwan Strait, Scavenging, Export flux

Citation: Wei, C. L., J. R. Tsai, Y. R. Hou, L. S. Wen, D. D. Sheu, and W. C. Chou, 2010: Scavenging phenomenon elucidated from  $^{234}\text{Th}/^{238}\text{U}$  disequilibrium in surface water of the Taiwan Strait. *Terr. Atmos. Ocean. Sci.*, 21, 713-726, doi: 10.3319/TAO.2009.08.26.01(Oc)

---

## 1. INTRODUCTION

The complexity of the coastal system is mainly due to strong and variable physical forcing and significant input of allochthonous materials from the landmass. The Taiwan Strait is a shallow shelf with an average depth of 60 m and serves as an important conduit for water exchange between the South China Sea and the East China Sea (Fig. 1). A large northward volume transport of 2.0 ~ 2.2 Sv was measured by Chung et al. (2001) and the transport is mainly through the Peng-Hu Channel (Jan and Chao 2003). Because this shallow and narrow water mass is bordered by the heavily populated China and Taiwan coastline, the Taiwan Strait receives large amounts of anthropogenic contaminants discharged from municipal areas through river inputs.

The combination of seismic activity and frequent typhoon results in extremely high sediment input from mountainous rivers of Taiwan. A total of 194 Mt  $\text{y}^{-1}$  fluvial sediments are carried into the Taiwan Strait by the mountainous

rivers of western Taiwan (Dadson et al. 2003). While seawater is fed from the south, it is conceivable that the fluvial sediments contributed from the rivers on both sides of the Taiwan Strait not only serve as an important source of terrestrial materials but also as an efficient scavenger and carrier for the particles and their associated trace elements and nutrients. To understand the fate of trace metals either carried from the south by the current or discharged from the land into the Taiwan Strait, it is essential to obtain more information on the rate of processes controlling the budgets of elements of interest. By using suitable naturally-occurring radionuclides, better knowledge regarding rates of processes governing trace element cycling in the Taiwan Strait can be greatly improved. Among those radionuclides, the short-lived  $^{234}\text{Th}$  ( $t_{1/2} = 24.1 \text{ d}$ ) is an ideal tracer for this purpose.

$^{234}\text{Th}$  is constantly produced from  $^{238}\text{U}$  in seawater. Once produced,  $^{234}\text{Th}$  is quickly attached to particle surfaces and removed from the water column. Depending on how fast  $^{234}\text{Th}$  is removed from a given parcel of seawater, the degree of deviation from secular equilibrium with  $^{238}\text{U}$

---

\* Corresponding author  
E-mail: weic@ntu.edu.tw

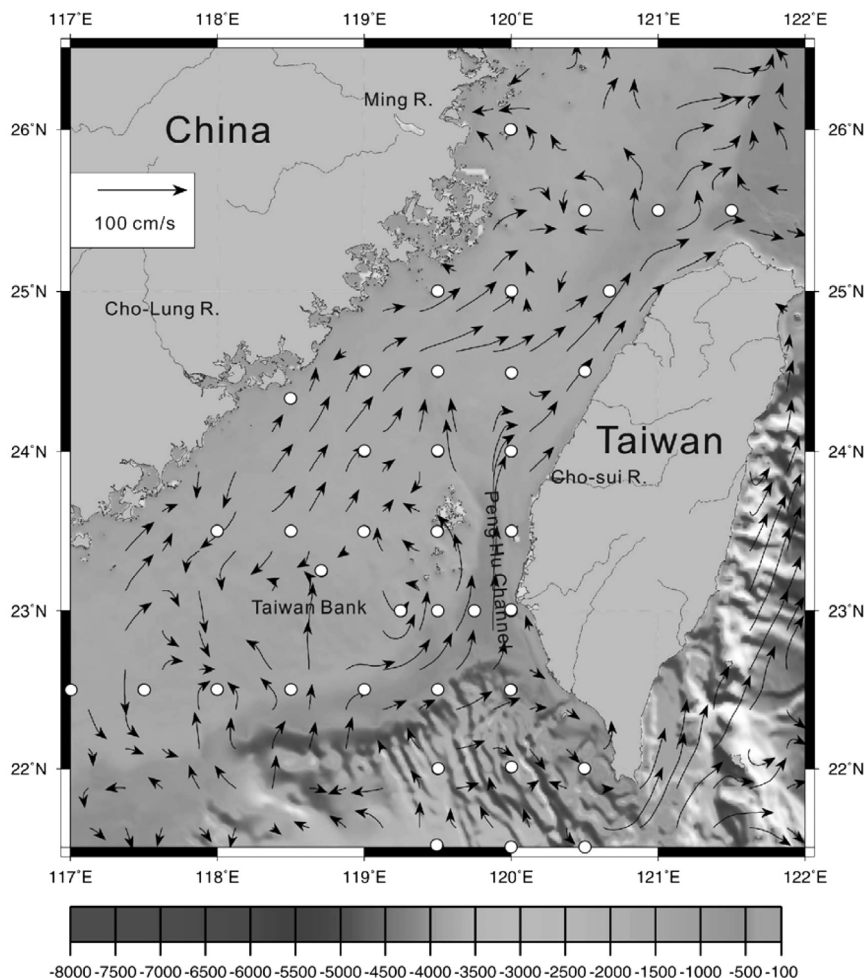


Fig. 1. Bathymetric map with large-volume sampling stations of the Taiwan Strait. Mean surface current calculated from shipboard May ADCP data collected during 1991 ~ 2006 are shown as vectors.

varies in different regimes of the ocean.  $^{234}\text{Th}/^{238}\text{U}$  disequilibrium is suitable for the investigation of scavenging and removal processes on timescales from days to weeks.  $^{234}\text{Th}$  has been widely used as a proxy of particulate organic carbon (Buesseler et al. 2006 and references therein), particulate inorganic carbon (Bacon et al. 1996), organic pollutants (Gustafsson et al. 1997), and trace metals (Weinstein and Moran 2005) to investigate elemental removal processes in the upper water column of the open oceans. However, due to the dynamic nature of coastal environments, there have been few studies applying the  $^{234}\text{Th}/^{238}\text{U}$  disequilibrium in coastal oceans (Santschi et al. 1979; Baskaran and Santschi 1993; Gustafsson et al. 1998; Benitez-Nelson et al. 2000; Radakovitch et al. 2003). To the best of our knowledge, no investigation of scavenging processes is available for the Taiwan Strait.

In May 2006, we took the opportunity of the Joint Hydrographic Survey launched by the National Center for Oceanographic Research of Taiwan (<http://www.ncor.ntu.edu.tw/odbs/JHS/index.html>, NCOR Report, 2006) to con-

duct seawater sampling in the Taiwan Strait for  $^{234}\text{Th}$  analyses. This paper aims to provide a quantitative estimate of scavenging and removal rates of  $^{234}\text{Th}$  by using  $^{234}\text{Th}/^{238}\text{U}$  disequilibrium.

## 2. MATERIALS AND METHODS

At the stations shown in Fig. 1, large-volume seawaters were sampled between 21 and 27 May 2006 as part of the Joint Hydrographic Survey project aboard three research vessels: the R/V Ocean Researcher I (cruise #796), the R/V Ocean Researcher II (cruise #1353), and the R/V Ocean Researcher III (cruise #1153). Seawater was collected at a depth of 2 meters using 10- or 20-L Teflon-coated Go-Flo bottles mounted on a Sea-Bird CTD (SBE 9/11) rosette assembly. A total of 38 large-volume (20 L) surface seawater samples were collected for the determination of dissolved ( $^{234}\text{Th}_d$ ) and particulate ( $^{234}\text{Th}_p$ )  $^{234}\text{Th}$ , and related hydrographic parameters (nutrients, particulate organic carbon and nitrogen).

## 2.1 Fluorescence and Light Transmission

Along the cruise track, continuous measurements of fluorescence and transmission were made by attaching a fluorometer and a transmissometer with 25 cm light path length on the underway system (Wetlabs C-Star) installed onboard. The intake of the underway system is about 2 meters below the surface.

## 2.2 Dissolved $^{234}\text{Th}$

Immediately after the seawater was transferred to the pressure drums, compressed air (at 12 p.s.i.) was used to pressure filter seawater through preweighed 142-mm Nuclepore filters (0.45  $\mu\text{m}$  pore size) mounted in a Plexiglas filter holder. The filters were rinsed with approximately 15 ml deionized distilled water to remove sea salt and stored in a petri dish to determine the total suspended matter (TSM) concentration and particulate  $^{234}\text{Th}$  activities.

The filtrate was acidified with about 20 ml concentrated HCl and spiked with 30 dpm of  $^{230}\text{Th}$  and 50 mg of Fe carrier. The samples were bubbled vigorously for at least 3 hours to help attain isotopic equilibration. Concentrated NaOH was then added to raise the pH to  $\sim 8$  to precipitate  $\text{Fe}(\text{OH})_3$ . The  $\text{Fe}(\text{OH})_3$  precipitates, with adsorbed thorium, were collected by siphoning and centrifugation, and then dissolved in concentrated HCl to a final concentration of 9 N HCl. These samples were then passed through an anion exchange column (Dowex IX-8) preconditioned with 9 N HCl to separate uranium from thorium. Thorium samples were purified by passing the sample through three anion exchange columns pre-conditioned with 8 N  $\text{HNO}_3$ . The sample was evaporated to incipient dryness and converted to a pH $\sim 1$  solution ready for Th extraction.  $^{234}\text{Th}$  and the yield tracer,  $^{230}\text{Th}$ , were extracted from the aqueous phase into a 0.4 M TTA (thenoyltrifluoroacetone)-benzene solution and the organic solvent was stippled on a stainless-steel disc. Preconcentration and separation of uranium and thorium from the filtered seawater samples were completed in three days after samples were collected.

## 2.3 TSM and Particulate $^{234}\text{Th}$

After weighing for the determination of TSM concentration, the filters were decomposed by soaking in  $\sim 10$  ml of concentrated  $\text{NH}_4\text{OH}$ . The samples were gently heated to evaporate the  $\text{NH}_4\text{OH}$  and then fluxed in  $\text{HClO}_4/\text{HF}$  to thoroughly digest organic and inorganic materials. After digestion, the samples were purified and mounted on stainless-steel discs following the same procedures as with dissolved  $^{234}\text{Th}$  samples.

The activities of  $^{234}\text{Th}$  were counted by a low background ( $< 0.15$  cpm) anticoincidence counter (Riso GM25-5) via its  $\beta$ -emitting daughter  $^{234}\text{Pa}$ . The counting efficiency

of the beta counter was regularly monitored by counting a  $^{238}\text{U}$  standard source. Chemical yield of thorium was estimated by counting spiked  $^{230}\text{Th}$  using silicon surface-barrier detectors (EG&G Ortec 576). The counting efficiencies of the  $\alpha$  detectors were calibrated against NIST traceable  $^{230}\text{Th}$  (Isotope Products Laboratory 387-67-3) standard plates. Activities of  $^{234}\text{Th}$  reported here were corrected back to the sampling time after the  $^{234}\text{Th}$  ingrown from  $^{238}\text{U}$  was subtracted.

## 2.4 Particulate Organic Carbon

Particulate organic carbon (POC) concentrations were determined by filtering 2 L seawater through precombusted (450°C) Whatman 25 mm GF/F filters. Filters were wrapped in aluminum foil and stored at  $-4^\circ\text{C}$ . In the laboratory the filters were acid-fumed to remove carbonates, and then analyzed for carbon and nitrogen with a Fisons elemental analyzer (NA1500). A calibration curve was obtained using acetanilide ( $\text{C}_8\text{H}_9\text{NO}$ ) as a standard. The overall procedural errors estimated from duplicate runs were better than  $\pm 2\%$  for carbon and nitrogen.

## 3. RESULTS

All data obtained from the bottle samples are given in Table 1 and shown as contour maps (Figs. 2 - 9). The distributions of surface temperature and salinity are shown in Figs. 2 and 3, respectively. They reveal the contribution of three water masses, the China Coastal Water (CCW), the Kuroshio Branch Water (KBW), and the South China Sea Surface Water (SCSSW). Generally, the hydrography in the Taiwan Strait is controlled by the interaction of the CCW originating from the north with either KBW or the SCSSW from the south. Due to persistent northward currents in the Taiwan Strait, the CCW, which is characterized by low temperature and low salinity, is limited to the northwestern Taiwan Strait. Significant freshening shown in the salinity distribution in the northwestern Taiwan Strait is evidently caused by the influence of riverine input from China coast. The KBW, with high temperature and high salinity, dominates the southeastern part of the Taiwan Strait and reaches as far north as to  $24^\circ 30'\text{N}$  in the coastal region of western Taiwan. With intermediate temperature and salinity values, the SCSSW occupies most part of the Taiwan Strait. As shown in Fig. 1, a strong and persistent current from the northeastern South China Sea through the Peng-Hu Channel can be seen (Jan and Chao 2003). Chung et al. (2001) concluded that the water mass in this northward current originated from the KBW in May and from the South China Sea Warm Water in August.

Distributions in surface water of fluorescence expressed as relative fluorescence units (RFU) and light beam attenuation coefficient (BAC) are shown in Figs. 4 and 5,

Table 1. Temperature, salinity, concentration of total suspended matter (TSM), dissolved ( $^{234}\text{Th}_d$ ) and particulate ( $^{234}\text{Th}_p$ )  $^{234}\text{Th}$  activities, and particulate organic carbon concentration obtained from the surface water of the Taiwan Strait. Standard deviations of  $^{234}\text{Th}_d$  and  $^{234}\text{Th}_p$  are based on propagated counting error (1 $\sigma$ ).

Station	Longitude °E	Latitude °N	Water Depth m	T °C	S psu	TSM mg L <sup>-1</sup>	$^{234}\text{Th}_d$ dpm L <sup>-1</sup>	$^{234}\text{Th}_p$ dpm L <sup>-1</sup>	POC μM
1	120.00	22.01	1111	27.83	34.266	0.30	1.39 ± 0.04	0.15 ± 0.01	-
2	119.50	22.00	2377	27.44	34.154	0.21	1.95 ± 0.05	0.16 ± 0.01	-
3	119.50	21.50	3003	27.49	34.145	0.22	1.47 ± 0.05	0.28 ± 0.02	-
4	120.00	21.50	2956	28.20	34.122	0.20	0.87 ± 0.02	0.16 ± 0.01	-
5	120.50	21.50	1736	28.89	33.983	0.20	0.97 ± 0.03	0.18 ± 0.01	-
6	120.50	22.00	1647	28.42	34.280	0.16	1.52 ± 0.03	0.11 ± 0.01	-
7	120.00	23.00	88	28.49	33.982	0.23	1.93 ± 0.00	0.24 ± 0.02	4.5
8	119.75	23.00	132	27.49	34.311	0.76	0.18 ± 0.02	0.60 ± 0.02	3.6
9	119.50	23.00	82	27.27	34.167	1.59	0.54 ± 0.01	0.46 ± 0.03	6.2
10	119.25	23.00	40	26.09	34.273	1.97	0.38 ± 0.01	0.42 ± 0.02	10.7
11	118.71	23.25	31	25.16	34.144	1.42	0.22 ± 0.02	0.34 ± 0.02	10.1
12	118.00	23.50	43	24.32	33.766	0.89	0.36 ± 0.06	0.46 ± 0.01	10.9
13	118.50	23.50	50	24.69	34.072	1.12	0.61 ± 0.01	0.45 ± 0.03	8.6
14	119.00	23.50	58	25.59	34.165	9.96	0.12 ± 0.01	0.30 ± 0.02	9.0
15	119.50	23.50	59	26.01	34.122	3.20	0.21 ± 0.01	0.45 ± 0.02	7.6
16	120.00	23.50	16	26.19	34.358	0.79	0.26 ± 0.01	0.65 ± 0.02	17.1
17	120.00	24.00	44	27.73	34.093	0.73	0.46 ± 0.01	0.39 ± 0.02	6.9
18	119.50	24.00	63	25.96	34.198	4.58	0.17 ± 0.00	0.45 ± 0.01	6.2
19	119.00	24.00	63	24.59	34.208	0.73	0.46 ± 0.01	0.39 ± 0.02	9.4
20	118.50	24.33	32	22.33	31.933	4.58	0.17 ± 0.06	0.45 ± 0.01	16.9
21	119.00	24.50	57	23.75	34.101	1.07	0.05 ± 0.01	0.23 ± 0.02	7.6
22	119.50	24.50	67	26.02	34.141	0.78	0.04 ± 0.01	0.27 ± 0.02	7.1
23	119.50	25.00	30	21.39	32.509	5.28	0.73 ± 0.00	0.22 ± 0.01	15.3
24	120.00	25.00	59	24.66	34.198	1.65	0.04 ± 0.01	0.28 ± 0.02	8.6
25	120.00	24.49	64	26.94	34.168	1.12	0.33 ± 0.01	0.34 ± 0.02	8.4
26	120.50	24.50	55	28.06	34.010	2.69	0.12 ± 0.02	0.30 ± 0.02	7.7
27	120.67	25.00	84	25.07	34.207	0.98	0.59 ± 0.01	0.30 ± 0.01	6.8
28	120.50	25.50	69	21.33	31.513	1.24	0.14 ± 0.01	0.15 ± 0.01	22.6
29	121.00	25.50	95	24.87	34.257	0.64	0.16 ± 0.00	0.21 ± 0.02	7.2
30	121.50	25.50	119	26.20	34.203	1.43	0.13 ± 0.01	0.34 ± 0.01	6.1
31	120.00	26.00	46	20.71	26.807	1.90	0.13 ± 0.00	0.14 ± 0.02	19.3
32	117.00	22.50	47	25.32	34.041	0.97	0.33 ± 0.01	0.43 ± 0.02	-
33	117.50	22.50	34	26.16	34.054	0.68	0.28 ± 0.01	0.42 ± 0.02	-
34	118.00	22.50	39	26.34	34.143	0.35	0.32 ± 0.01	0.46 ± 0.03	-
35	118.50	22.50	66	26.47	34.141	0.47	0.34 ± 0.01	0.43 ± 0.03	-
36	119.00	22.50	89	27.15	34.182	0.20	0.67 ± 0.02	0.21 ± 0.01	-
37	119.50	22.50	229	27.29	34.166	0.16	1.58 ± 0.04	0.41 ± 0.03	-
38	120.00	22.50	629	28.44	34.013	0.17	1.36 ± 0.05	0.47 ± 0.03	-

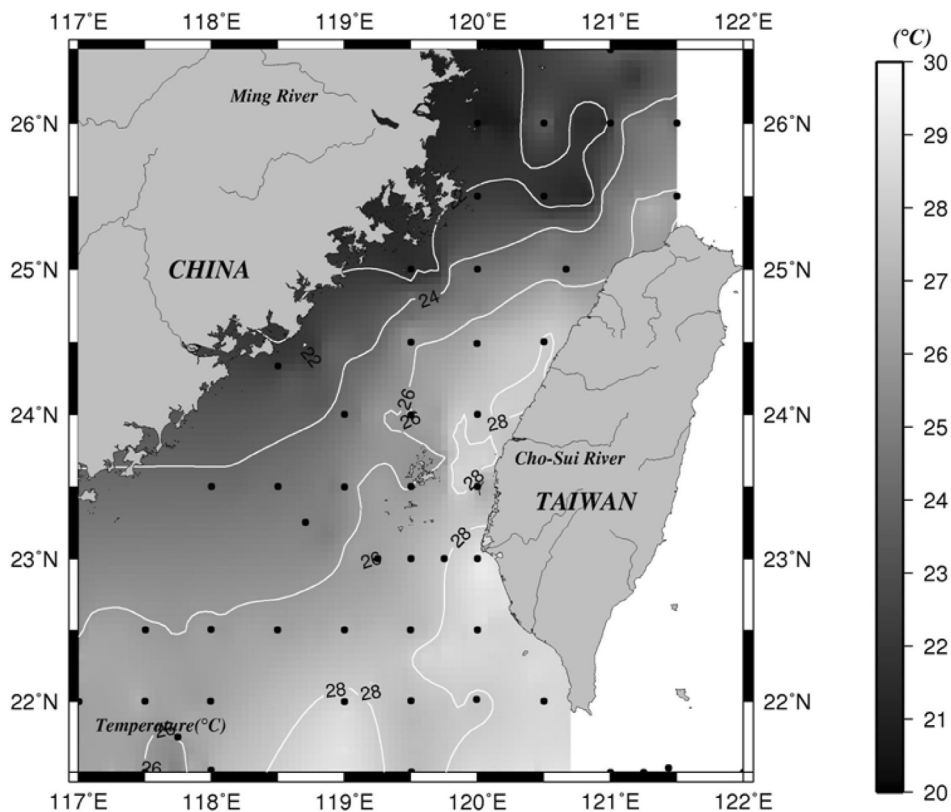


Fig. 2. Distribution of temperature in surface water of the Taiwan Strait.

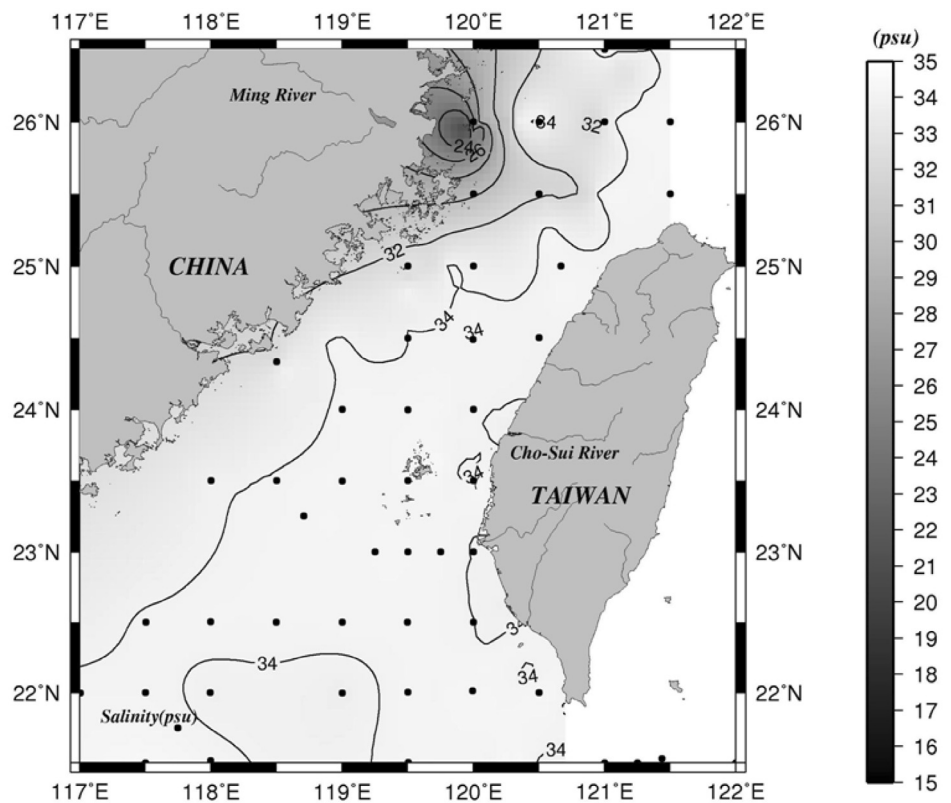


Fig. 3. Distribution of salinity in surface water of the Taiwan Strait.

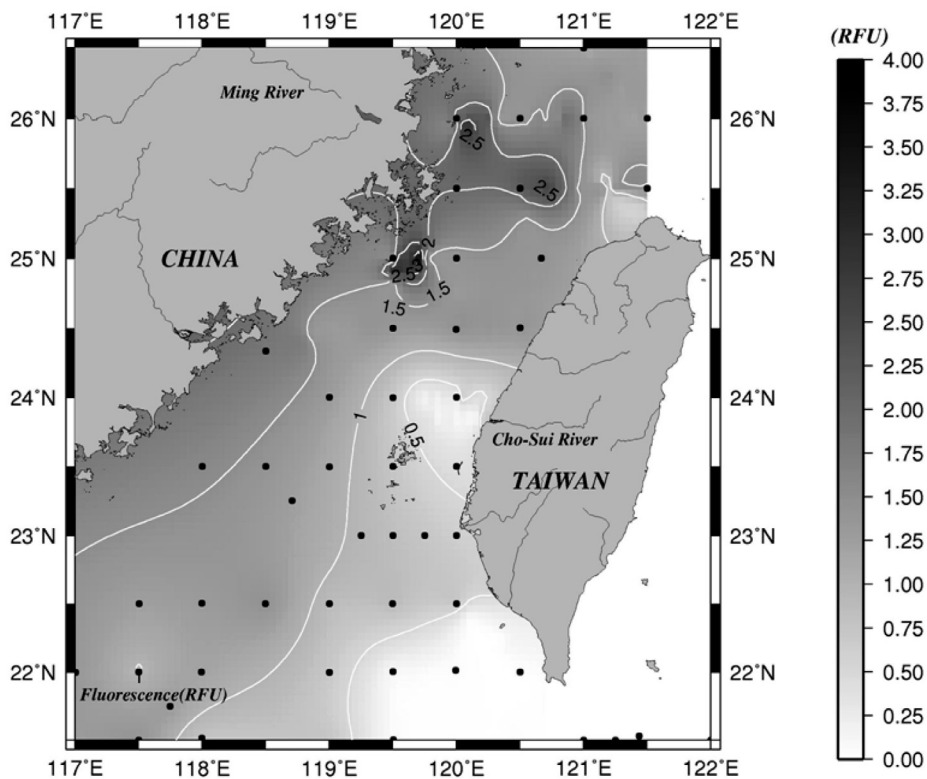


Fig. 4. Distribution of relative fluorescence unit (RFU) in surface water of the Taiwan Strait. RFU was measured by fluorometer attached to the underway system during the cruises.

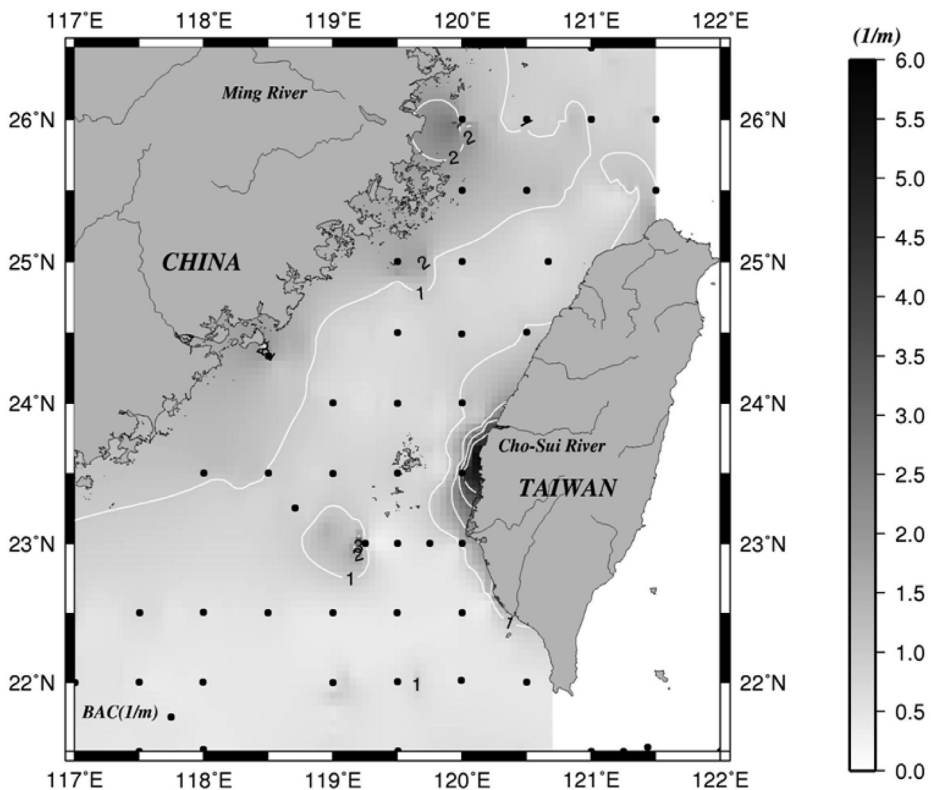


Fig. 5. Distributions of beam light attenuation coefficient (BAC) in surface water of the Taiwan Strait. BAC was measured by transmissometer attached to the underway system during the cruises.

respectively. Generally, the distribution of fluorescence reflects the geographic distribution of chlorophyll concentration. We found higher RFU values in the western and northern portions of the Taiwan Strait. Higher fluorescence water was associated with higher silicate concentration (data not shown). The distribution of fluorescence followed the pattern in concentration of total pigments measured using HPLC in samples collected from the same stations as this study (Tung 2007). The highest and lowest biomasses were found in the Ming River mouth and Cho-Sui River mouth, respectively. According to Tung (2007), the chlorophyll biomass is mostly (> 80%) contributed by diatoms in the region of the Ming River and Cho-Lung River mouths.

The distribution of BAC essentially reflected the geographical variability of TSM, as shown in Fig. 6, and showed a positive relationship between TSM and BAC:  $TSM (mg L^{-1}) = 2.40 \times BAC (m^{-1}) - 0.75$ ,  $R^2 = 0.88$ ,  $n = 64$ . In the vicinity of the Cho-Sui River mouth, the BAC was the highest, indicating fluvial sediment input. The BAC in the mouth of the Ming River mouth showed elevated values, whereas the TSM distribution in the general area remained low. Because the beam attenuation coefficient is also affected by colored dissolved substances (Zaneveld 1994), elevated BAC in the vicinity of Ming River mouth may have been caused by fluvial input of dissolved substances rather than by absorption and scattering by particles. Indeed, Hung et al. (2000; 2003) observed a water mass of high dissolved organic carbon (> 90  $\mu m$ ) in the vicinity of the Ming River mouth. Not surprisingly, TSM concentration was higher in

the vicinity of Cho-Sui River mouth and in the coastal water of China. In contrast, clearer water from the South China Sea dominated the southern Taiwan Strait.

The distribution of POC in the study region is shown in Fig. 7. Generally, the POC concentration was higher in the western than in the eastern Taiwan Strait. It is evident that the POC concentration increases in areas under the influence of riverine inputs. No POC data were measured south of 23°N, but POC concentration ranging between 8.8 and 16.3  $\mu m$  were observed by Kao et al. (2006) in the surface water off southwestern Taiwan, indicating the POC concentrations in the southern part of the Taiwan Strait may have been similar to that in the eastern side of the strait.

Contours for activities of dissolved ( $^{234}Th_d$ ) and particulate ( $^{234}Th_p$ )  $^{234}Th$  are shown in Figs. 8 and 9, respectively. The spatial distribution of  $^{234}Th_d$  corroborates the circulation pattern in the Taiwan Strait. A relatively high  $^{234}Th_d$  is associated with the KBC and extends northward through the Peng-Hu Channel. The  $^{234}Th_d$  in the shallow shelf of the study area showed very low values (< 0.5 dpm  $L^{-1}$ ). Unlike the  $^{234}Th_d$  distribution, the  $^{234}Th_p$  showed low values in the regions of the Ming River mouth and off southwestern Taiwan. In contrast, a patch of high  $^{234}Th_p$  water was indicated in the vicinity of the Cho-Sui River mouth.

#### 4. DISCUSSION

Due to the highly particle-reactive characteristics,  $^{234}Th$  is rapidly removed from seawater to the extent that a large

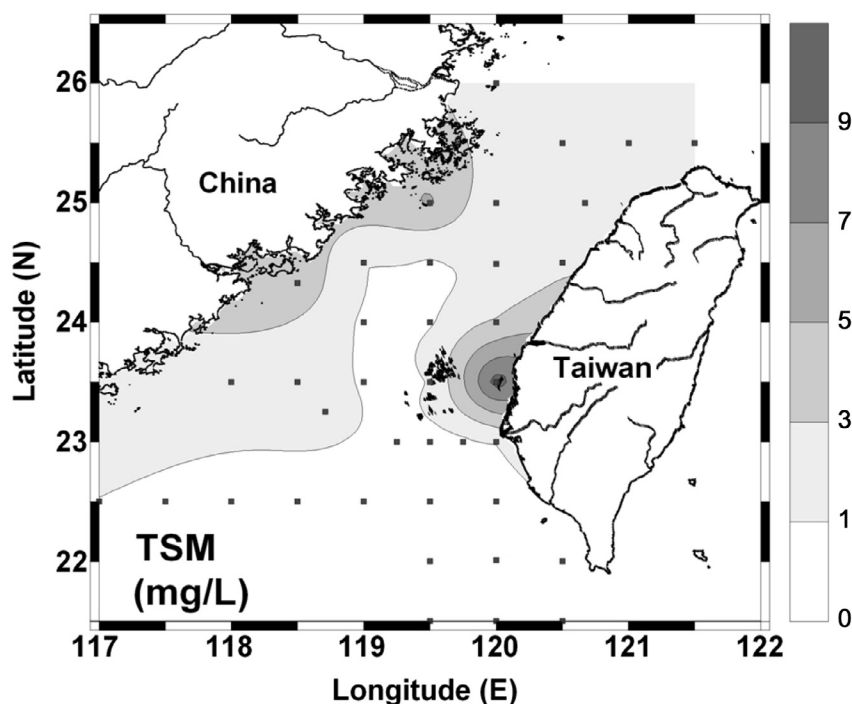


Fig. 6. Distribution of total suspended matter (TSM) concentration in surface water of the Taiwan Strait.

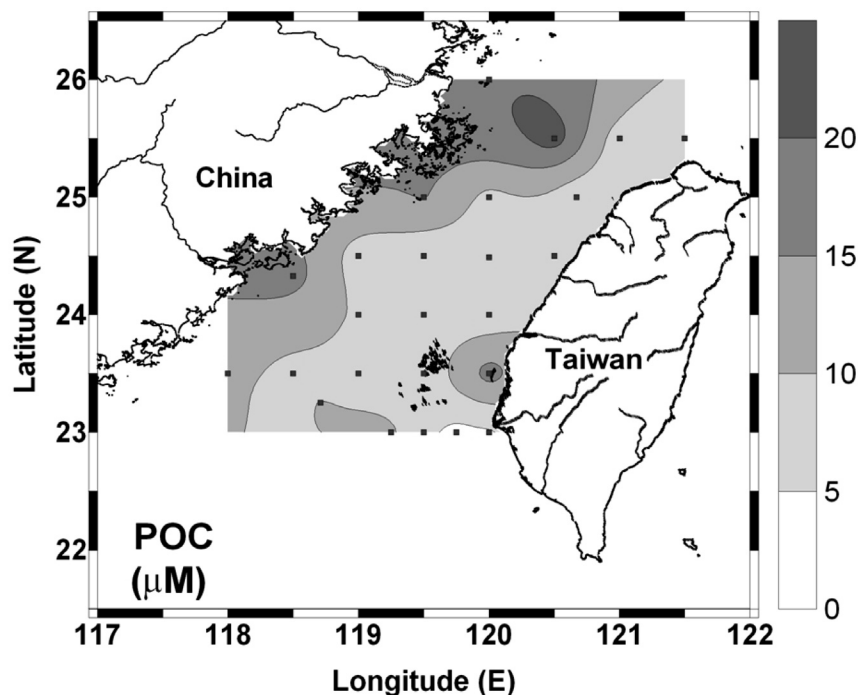


Fig. 7. Distribution of particulate organic carbon in surface water of the Taiwan Strait.

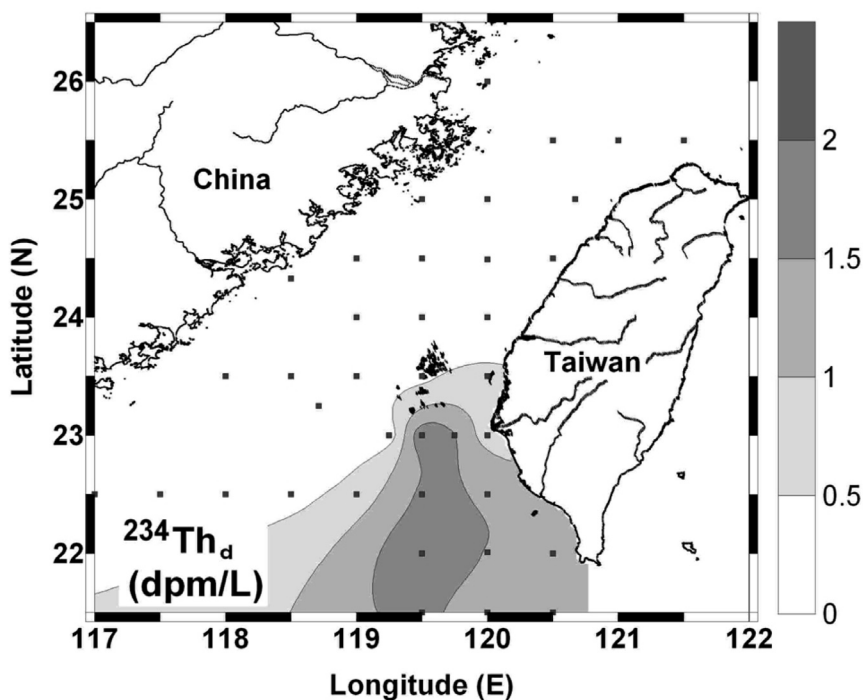


Fig. 8. Distribution of dissolved  $^{234}\text{Th}$  in surface water of the Taiwan Strait.

deficiency from secular equilibrium with  $^{238}\text{U}$ , especially in the shallow shelf region of the Taiwan Strait. The  $^{238}\text{U}$  activity in the coastal water off western Taiwan follows the salinity- $^{238}\text{U}$  relationship of Ku et al. (1977),  $^{238}\text{U}$  ( $\text{dpm L}^{-1}$ ) =  $0.07081 \times \text{Salinity}$  (unpublished results). Accordingly, this

relationship was used to calculate  $^{238}\text{U}$  activity from the salinity data. The ratio of total (dissolved + particulate)  $^{234}\text{Th}$  to  $^{238}\text{U}$  at most of our sampling stations were lower than 0.4, indicating that removal of  $^{234}\text{Th}$  was faster than supply by mixing of different water mass in the Taiwan Strait.

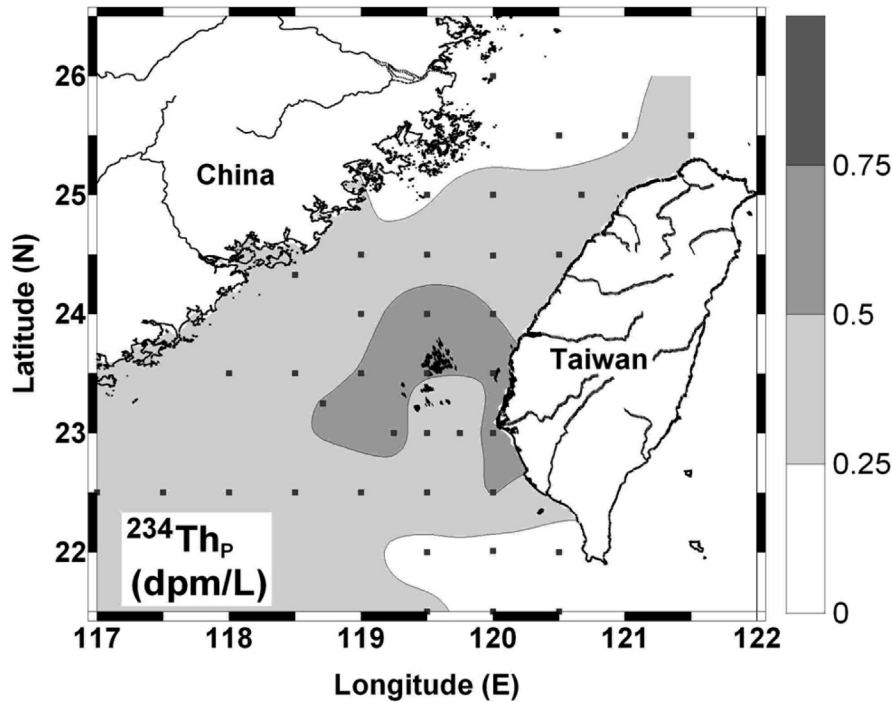


Fig. 9. Distribution of particulate  $^{234}\text{Th}$  in surface water of the Taiwan Strait.

Since the simple irreversible scavenging model was first used for estimating the scavenging and removal rates of  $^{234}\text{Th}$  in seawater (Coale and Bruland 1985), the oceanographic research community has needed for a more realistic model for the  $^{234}\text{Th}$  budget in the ocean. To understand the behavior of  $^{234}\text{Th}$  in a dynamic environment, where advective transport may significantly control the distribution of  $^{234}\text{Th}$ , the model should account for physical mixing processes (Benitez-Nelson et al. 2000; Buesseler et al. 2006). Similar to the model used by Wei et al. (2009), assuming a steady-state, the mass balance of  $^{234}\text{Th}_d$  and  $^{234}\text{Th}_p$  are described by the following equations,

$$\frac{d^{234}\text{Th}_d^i}{dt} = 0 = \frac{V_i(^{234}\text{Th}_{d^{i-1}} - ^{234}\text{Th}_d^i)}{\Delta L} + \lambda U_i - \lambda ^{234}\text{Th}_d^i - J_i \quad (1)$$

$$\frac{d^{234}\text{Th}_p^i}{dt} = 0 = J_i + \frac{V_i(^{234}\text{Th}_{p^{i-1}} - ^{234}\text{Th}_p^i)}{\Delta L} - \lambda ^{234}\text{Th}_p^i - P_i \quad (2)$$

Where,

$U_i$  =  $^{238}\text{U}$  activity in the  $i$ -th box ( $\text{dpm m}^{-3}$ );

$^{234}\text{Th}_d^i$  = dissolved  $^{234}\text{Th}$  activity in the  $i$ -th box ( $\text{dpm m}^{-3}$ );

$^{234}\text{Th}_p^i$  = particulate  $^{234}\text{Th}$  activity in the  $i$ -th box ( $\text{dpm m}^{-3}$ );

$V_i$  = average current velocity in the  $i$ -th box ( $\text{m d}^{-1}$ );

$\Delta L$  = distance between the centers of consecutive boxes (m);

$\lambda$  = radioactive decay constant of  $^{234}\text{Th}$  ( $\text{d}^{-1}$ );

$J_i$  = net change rate of dissolved  $^{234}\text{Th}$  due to scavenging process in the  $i$ -th box ( $\text{dpm m}^{-3} \text{d}^{-1}$ ); and

$P_i$  = net change rate of particulate  $^{234}\text{Th}$  due to particle removal process in the  $i$ -th box ( $\text{dpm m}^{-3} \text{d}^{-1}$ ).

In the model, the particulate phase is assumed to be transported by current because fine particles remain in suspension in this dynamic system of strong advection. The residence times of dissolved ( $\tau_d$ ) and particulate ( $\tau_p$ )  $^{234}\text{Th}$  with respect to scavenging and particle removal, respectively, can be calculated by:

$$\tau_d = \frac{^{234}\text{Th}_d}{J} \quad (3)$$

$$\tau_p = \frac{^{234}\text{Th}_p}{P} \quad (4)$$

Based on the environmental settings and the spatial distribution of  $^{234}\text{Th}_d$  and  $^{234}\text{Th}_p$ , the study area was divided into five boxes (Fig. 10) and treated as an advection-scavenging-removal system. Following the procedures of Liang et al. (2003), the mean current velocity in May at the boundary of each box was estimated by averaging archived shipboard ADCP data (NCOR Data Bank) collected during 1991 ~ 2006. In each box, the number of ADCP data sets for averaging current velocity ranges from 2400 to 3115, which gives a root mean square (rms) error of  $\sim 5 \text{ cm s}^{-1}$  (Liang et al. 2003).

The results of the model calculation on dissolved and particulate  $^{234}\text{Th}$  for the five areas are shown in Table 2. Since both ADCP and current meter data collected from the Luzon Strait showed a persistent and strong flow of Kuroshio Branch Water through the northern Luzon Strait into the region off southwestern Taiwan (Liang et al. 2003), we used 1.5 and 0.25 dpm  $\text{L}^{-1}$ , respectively, as the  $^{234}\text{Th}_d$  and  $^{234}\text{Th}_p$  of influx water into Box I (Wei and Hung 1992). The average  $^{234}\text{Th}_d$  and  $^{234}\text{Th}_p$  activities of the influx water to Box II were  $1.0 \pm 0.2$  and  $0.2 \pm 0.04$  dpm  $\text{L}^{-1}$ , respectively, which were measured at the station ( $118^\circ 00' \text{E}$ ,  $22^\circ 18' \text{N}$ ) in the northern South China Sea (unpublished results).

Depending on the average current velocity and the differences of  $^{234}\text{Th}_d$  and  $^{234}\text{Th}_p$  between adjacent boxes, the

contributions of physical transport to the  $^{234}\text{Th}_d$  and  $^{234}\text{Th}_p$  mass balance vary from -40 to 643 dpm  $\text{m}^{-3} \text{d}^{-1}$  for  $^{234}\text{Th}_d$  and from -128 to 86 dpm  $\text{m}^{-3} \text{d}^{-1}$  for  $^{234}\text{Th}_p$ . Positive values indicate that more  $^{234}\text{Th}$  was imported than exported from the box, whereas negative values indicate the amount of  $^{234}\text{Th}$  imported to the box was less than the amount exported. The percentage of advection to the P value ranges from 21% in Box II to 36% in Box IV. Since the advection term in Eq. (2) was significantly smaller than the particle removal term, it is reasonable to conclude that vertical processes for  $^{234}\text{Th}$  removal were more important than horizontal transport. Not surprisingly, physical transport causes the largest effect on the  $^{234}\text{Th}$  budget in the central part of the Taiwan Strait (Boxes III and IV) because a large amount of dissolved  $^{234}\text{Th}$  was

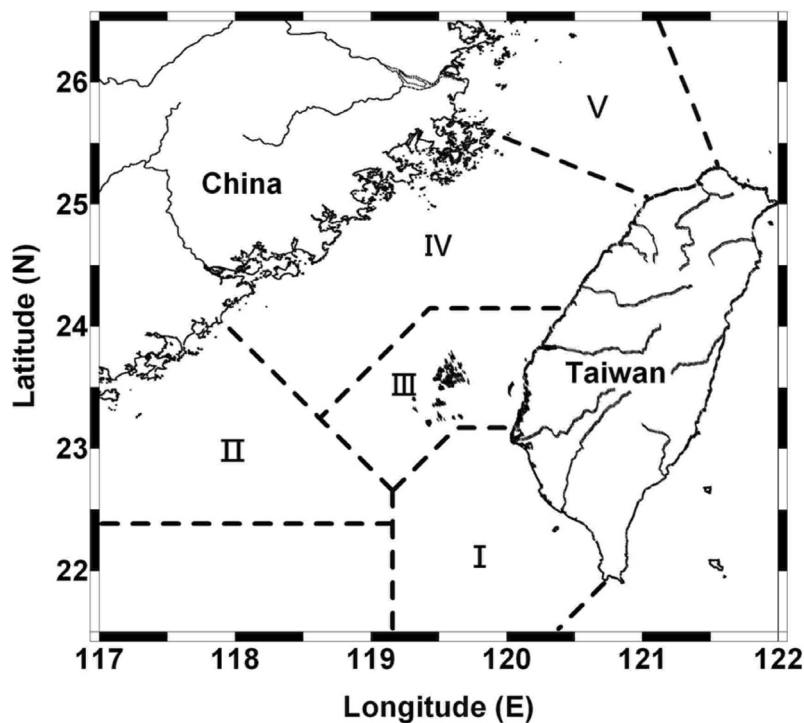


Fig. 10. Five regions in the Taiwan Strait delineated for the model calculation.

Table 2. Parameters used and the results of the advective-scavenging-removal model for the five domains in the Taiwan Strait.

Box	$^{234}\text{Th}_d$	$^{234}\text{Th}_p$	J	P	$\tau_d$	$\tau_p$	POC/ $^{234}\text{Th}$	$F_{\text{POC}}$	$\tau_{\text{POC}}$
	dpm $\text{L}^{-1}$		dpm $\text{m}^{-3} \text{d}^{-1}$		day		$\mu\text{mol dpm}^{-1}$	$\text{mmol m}^{-3} \text{d}^{-1}$	day
I	$1.59 \pm 0.23$	$0.26 \pm 0.13$	$32 \pm 61$	$24 \pm 77$	$50 \pm 12$	$11 \pm 1$	$13.5 \pm 8.2$	$0.3 \pm 1.5$	$15 \pm 2$
II	$0.36 \pm 0.14$	$0.39 \pm 0.09$	$125 \pm 31$	$94 \pm 35$	$3 \pm 3$	$4 \pm 24$	$23.7 \pm 4.6$	$2.2 \pm 0.8$	$4 \pm 26$
III	$0.32 \pm 0.16$	$0.51 \pm 0.09$	$703 \pm 133$	$560 \pm 150$	$0 \pm 0$	$1 \pm 1$	$18.1 \pm 8.9$	$10.2 \pm 3.5$	$1 \pm 1$
IV	$0.06 \pm 0.04$	$0.27 \pm 0.03$	$159 \pm 61$	$237 \pm 76$	$0 \pm 0$	$1 \pm 0$	$29.4 \pm 13.1$	$7.0 \pm 3.7$	$1 \pm 1$
V	$0.14 \pm 0.02$	$0.21 \pm 0.09$	$53 \pm 9$	$64 \pm 20$	$3 \pm 1$	$3 \pm 1$	$66.1 \pm 49.7$	$4.2 \pm 4.0$	$3 \pm 3$

carried into the Taiwan Strait by the strong current through the Peng-Hu Channel (Fig. 1). Note that the advection term for  $^{234}\text{Th}_d$  in Box III exceeds the *in situ*  $^{234}\text{Th}$  production from  $^{238}\text{U}$  decay ( $\sim 70 \text{ dpm m}^{-3} \text{ d}^{-1}$ ) by a factor of 9.

Although the advection terms were significant in each box, they were generally smaller than the scavenging [J in Eq. (1)] and particle removal [P in Eq. (2)] terms. Since only  $^{234}\text{Th}_d$  and  $^{234}\text{Th}_p$  in the surface water were determined, removal rates in  $\text{dpm m}^{-3} \text{ d}^{-1}$  rather than fluxes in  $\text{dpm m}^{-2} \text{ d}^{-1}$ , which requires knowledge of vertical profiles of  $^{234}\text{Th}$ , are reported here. Relating to the biochemical settings of each domain, the J ranges from  $32 \text{ dpm m}^{-3} \text{ d}^{-1}$  in Box I to  $703 \text{ dpm m}^{-3} \text{ d}^{-1}$  in Box III and the P ranges from  $24 \text{ dpm m}^{-3} \text{ d}^{-1}$  in Box II to 560 in Box III.

Box I represents the only domain deeper than 200 m in the Taiwan Strait and can illustrate the hydrographic characteristics of Kuroshio Branch Current. A scavenging rate of  $32 \text{ dpm m}^{-3} \text{ d}^{-1}$  and particle removal rate of  $24 \text{ dpm m}^{-3} \text{ d}^{-1}$  were obtained from the model calculations, which result in residence times of 50 and 11 days for dissolved  $^{234}\text{Th}$  and particulate  $^{234}\text{Th}$ , respectively. The model results imply that  $^{234}\text{Th}$  cycling in this region is limited by the scavenging rate and, once scavenged onto particles,  $^{234}\text{Th}$  is removed vertically from the surface water in a short period of time.

Box II encloses the Taiwan Bank, a shallow area of only 20 m average depth. An eddy covering the Taiwan Bank (Fig. 1) may enhance the suspension of particles. The  $^{234}\text{Th}_d$  and  $^{234}\text{Th}_p$  data in Box II also indicated relatively homogeneous distribution, supporting enhanced mixing due to the eddy. In contrast to Box I, the J term is larger than the P term in Box II, implying that particle settling was inhibited by strong tidal forcing. Thus our data suggest a short particulate  $^{234}\text{Th}$  residence time of only 1 day. Both the highest scavenging and removal rates derived from the model were found in Box III. As shown in the  $^{234}\text{Th}_d$  contour map, northward transport of South China Sea water brings in large amount of  $^{234}\text{Th}$  through the Peng-Hu Channel. The role of Cho-Sui River can be seen from the distribution of  $^{234}\text{Th}_p$ , which was dramatically elevated around  $23 \sim 24^\circ\text{N}$  in the eastern Taiwan Strait. Terrestrial materials brought in by the Cho-Sui River scavenge thorium from seawater to cause the distinct patch of elevated  $^{234}\text{Th}_p$  in the map. Among many rivers of the western Taiwan, the Cho-Sui River is the largest source of fluvial sediments to the Taiwan Strait. The annual sediment input of Cho-Sui River is 64 Mt, accounting for 70% of total sediment transportation by western Taiwanese rivers (Dadson et al. 2003). This large fluvial input serves as an efficient interceptor for particle-reactive elements transported from the south. The high P value found in Box III is conceivable based on the fact that fast settling coarse sediments from the Cho-Sui River quickly remove  $^{234}\text{Th}$  from the water column. Residence times of dissolved and particulate  $^{234}\text{Th}$  with respect to scavenging and particle removal are short, one day.

Box V covers the region affected by Ming River input, in which both  $^{234}\text{Th}_d$  and  $^{234}\text{Th}_p$  are low (Figs. 8 and 9). Among the five boxes, the scavenging rate in this domain is comparable with that in Box I,  $53 \text{ dpm m}^{-3} \text{ d}^{-1}$ , and the particle removal rate is relatively low,  $64 \text{ dpm m}^{-3} \text{ d}^{-1}$ . The relatively low J is attributed to the high concentration of dissolved organic matter in the region. Hung et al. (2000) observed a high concentration ( $80 \sim 119 \mu\text{M}$ ) of DOC, of which  $\sim 27\%$  is in the colloidal form ( $> 1 \text{ kDa}$ ), in the region near the Ming River. High dissolved organic materials provide more complexing ligands for retaining thorium in the dissolved phase (Santschi et al. 2003).

Here we use  $^{234}\text{Th}$  as a proxy of organic carbon to estimate the removal rate of POC via particle settling in the Taiwan Strait. Removal rates of POC ( $F_{\text{POC}}$ ) were calculated by  $P_i \times (\text{POC}/^{234}\text{Th})_i$ , where  $(\text{POC}/^{234}\text{Th})_i$  is the ratio of particulate organic carbon to particulate  $^{234}\text{Th}$  in suspended particles in box i. Before we proceed, some reflection of this application may be in order. Although  $^{234}\text{Th}$  has been extensively used as a proxy of POC, large uncertainty arising from the variability of the  $\text{POC}/^{234}\text{Th}$  ratio in the oceans has been found. Buesseler et al. (2006) discussed the factors that may cause variability of  $\text{POC}/^{234}\text{Th}$  ratios in particles, including size, composition, shape, morphology, and sinking velocity of particles. Different sampling techniques have been used to collect marine particles for the determination of the  $\text{POC}/^{234}\text{Th}$  ratio. Many used large-volume *in situ* pump and chose the  $\text{POC}/^{234}\text{Th}$  ratio in  $> 53 \mu\text{m}$  particles as representative value for POC export calculation (Buesseler et al. 1995; Bacon et al. 1996; Hung et al. 2004), while others, including those involved in the JGOFS EqPac program (e.g., Murray et al. 1996), considered the ratio determined from the sinking particles directly collected by sediment traps at the euphotic depth to be the most suitable  $\text{POC}/^{234}\text{Th}$  ratio for  $^{234}\text{Th}$  proxy approach of POC export. The  $\text{POC}/^{234}\text{Th}$  ratio in sinking particles was not available in this study; however, our measurements in the northern South China Sea and the Kuroshio showed that the  $\text{POC}/^{234}\text{Th}$  ratio of  $0.45 - 10 \mu\text{m}$  particles ( $15 \sim 20 \mu\text{mol dpm}^{-1}$ ) is fairly similar to that in sinking particles ( $10 \sim 15 \mu\text{mol dpm}^{-1}$ ) collected by floating traps. On the other hand, the  $\text{POC}/^{234}\text{Th}$  ratio in suspended particles of larger sizes ( $10 - 63, 63 - 153, > 153 \mu\text{m}$ ) is 3  $\sim$  8 fold higher than that in sinking particles. The similar  $\text{POC}/^{234}\text{Th}$  ratio between fine ( $0.45 - 10 \mu\text{m}$ ), suspended particles and sinking particles indicates little fractionation of carbon and  $^{234}\text{Th}$  during particle aggregation processes. Though we are aware of the caveats of utilizing  $^{234}\text{Th}$  as POC proxy for estimating export, we argue that the results collected using conventional filtration of seawater through  $0.45 \mu\text{m}$  filters can provide a first-order approximation of scavenging process in the Taiwan Strait.

The  $\text{POC}/^{234}\text{Th}_i$  ratios in the Taiwan Strait do exhibit large variations, ranging between 8 to  $154 \mu\text{mol dpm}^{-1}$

(Fig. 11). Benitez-Nelson et al. (2000) also observed a large range of POC/ $^{234}\text{Th}$  ratio, from 2 to 534  $\mu\text{mol dpm}^{-1}$ , with most values  $> 10 \mu\text{mol dpm}^{-1}$ , in filtered particles collected from the surface water of the Gulf of Maine. Variation in biogeochemical settings may be responsible for the high variability of POC/ $^{234}\text{Th}$  ratio in the Taiwan Strait. Specific concentration of organic carbon in the suspended particles shows higher abundance of organic-rich particles along the China coast, which may be caused by enhanced growth of biological particles induced from terrestrial input of nutrients. The biomass in the domain covered by Box V is dominated by diatoms (Tung 2007). The highest POC/ $^{234}\text{Th}$  in the northwestern Taiwan Strait can reach values as high as 154  $\mu\text{mol dpm}^{-1}$ , implying that planktons grown in the region are larger in size. These carbon-enriched meso- to macroplanktons, with smaller surface to volume ratios, provide lower surface areas for thorium scavenging. In contrast, POC/ $^{234}\text{Th}$  is much lower in the southern Taiwan Strait, suggesting that plankton residing in the South China Sea seawater are smaller in size due to the oligotrophic nature of the water mass. Tung (2007) found the dominant plankton in this region is cyanobacteria. Our results showed that the lowest POC/ $^{234}\text{Th}$  was found in Box III, the region under the influence of the Cho-Sui River, with large amounts of detrital material containing less organic carbon and hence low in POC/ $^{234}\text{Th}$ .

The average POC/ $^{234}\text{Th}$  ratio, the POC removal rate and the residence time of POC ( $\tau_{\text{POC}}$ ) in the five areas of

the Taiwan Strait are shown in Table 2. Errors ( $\pm 1\sigma$ ) were propagated from uncertainties associated with measured and estimated parameters. The removal rate of POC from the surface water of the Taiwan Strait ranges from 0.3 ~ 10.2  $\text{mmol-C m}^{-3} \text{d}^{-1}$ . Generally, the POC removal rate in the southern Taiwan Strait is lower than that in the northern Taiwan Strait. The Relatively low POC removal rate in the Taiwan Bank, 2.2  $\text{mmol-C m}^{-3} \text{d}^{-1}$ , may be a result of resuspension in this shallow region with an average water depth of 20 m. In comparison with the primary productivity of 1.1 ~ 2.1  $\text{mmol-C m}^{-3} \text{d}^{-1}$  in this region (Huang et al. 1999), most POC produced in the surface is exported to the deep layer. With respect to the removal rate, the residence time of POC in the Taiwan Strait ranges from 1 day in Boxes III and IV to 15 days in Box I. The POC residence time with respect to particle removal in Box V is  $3 \pm 3$  days. This estimate of POC residence time is comparable with Hung et al. (2000), who found a residence time of 6 days for POC estimated from the ratio of the POC inventory in the euphotic layer and the rate of new production in the inner shelf of the southern East China Sea, the region immediately to the north of our Box V.

## 5. CONCLUSIONS

From the distribution of dissolved and particulate  $^{234}\text{Th}$  we made a quantitative estimate of the scavenging and particle removal rates in the surface water of the Taiwan Strait.

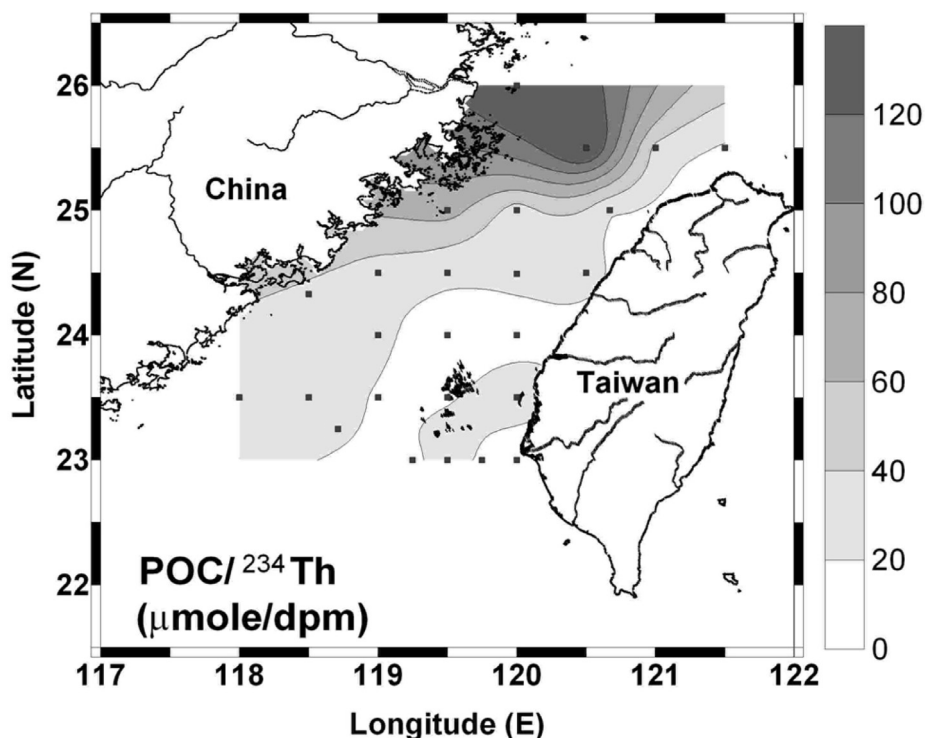


Fig. 11. Distribution of the ratio of particulate organic carbon to particulate  $^{234}\text{Th}$  (POC/ $^{234}\text{Th}$ ) in surface water of the Taiwan Strait.

Multiplying the POC/ $^{234}\text{Th}$  ratio by the particle removal rate estimated from  $^{234}\text{Th}/^{238}\text{U}$  disequilibrium, the removal rate of particulate organic carbon from the surface water of the Taiwan Strait was also estimated. Based on the environmental settings (hydrography and topography), the Taiwan Strait was divided into five regimes for our model manipulation. The calculated results are summarized as follows:

- (1) Occupied by the Kuroshio Branch Water, region 1 has higher temperature and salinity. This region has the highest scavenging and removal rates of  $^{234}\text{Th}$ , with  $\tau_d = 50$  and  $\tau_p = 11$  days, similar to open ocean values.
- (2) Overlying the Taiwan Bank, region 2 has the lowest scavenging and removal rates due to resuspension of bottom sediments in this shallow region. The removal rate of POC from the surface water in this region is therefore relatively low,  $2.2 \pm 0.8 \text{ mmol-C m}^{-3} \text{ d}^{-1}$ .
- (3) Covering the Cho-Sui River's mouth, region 3 has extremely high particle concentration. Therefore,  $^{234}\text{Th}$  is scavenged and removed at a very fast rate, with  $\tau_d$  and  $\tau_p$  of one day only.
- (4) In the middle of Taiwan Strait, region 4 has relatively high scavenging and particle removal rates, hence a short  $\tau_d$  and  $\tau_p$  of  $\leq 1$  day.
- (5) Encompassing the Ming River's mouth, region 5 is characterized by low temperature, low salinity and high chlorophyll-a. In this region both  $\tau_d$  and  $\tau_p$  are  $\sim 3$  days.

**Acknowledgements** We acknowledge the NCOR Data Bank for providing us valuable historical ADCP data. We thank the help from Y. H. Wang for ADCP data processing and H. S. Wang for underway data processing. Help provided by the captains and crew of R/Vs Ocean Researcher I, II, and III is appreciated. Constructive comments by Drs. Peter Santschi and Shangde Luo significantly helped improve the paper. This research was supported by NSC through grant NSC-95-2611-M-002-012.

## REFERENCES

- Bacon, M. P., J. K. Cochran, D. Hirschberg, T. R. Hammar, and A. P. Fleer, 1996: Export flux of carbon at the equator during the EqPac time-series cruises estimated from  $^{234}\text{Th}$  measurements. *Deep-Sea Res. II*, **43**, 1133-1153, doi: 10.1016/0967-0645(96)00016-1. [[Link](#)]
- Baskaran, M. and P. H. Santschi, 1993: The role of particles and colloids in the transport of radionuclides in coastal environments of Texas. *Mar. Chem.*, **43**, 95-114, doi: 10.1016/0304-4203(93)90218-D. [[Link](#)]
- Benitez-Nelson, C. R., K. O. Buesseler, and G. Crossin, 2000: Upper ocean carbon export, horizontal transport, and vertical eddy diffusivity in the southwestern Gulf of Maine. *Cont. Shelf Res.*, **20**, 707-736, doi: 10.1016/S0278-4343(99)00093-X. [[Link](#)]
- Buesseler, K. O., J. A. Andrews, M. C. Hartman, R. Be-  
lastock, and F. Chai, 1995: Regional estimates of the export flux of particulate organic carbon derived from thorium-234 during the JGOFS EqPac program. *Deep-Sea Res. II*, **42**, 777-804, doi: 10.1016/0967-0645(95)00043-P. [[Link](#)]
- Buesseler, K. O., C. R. Benitez-Nelson, S. B. Moran, A. Burd, M. Charette, J. K. Cochran, L. Coppola, N. S. Fisher, S. W. Fowler, W. D. Gardner, L. D. Guo, O. Gustafsson, C. Lamborg, P. Masque, J. C. Miquel, U. Passow, P. H. Santschi, N. Savoye, G. Stewart, and T. Trull, 2006: An assessment of particulate organic carbon to thorium-234 ratios in the ocean and their impact on the application of  $^{234}\text{Th}$  as a POC flux proxy. *Mar. Chem.*, **100**, 213-233, doi: 10.1016/j.marchem.2005.10.013. [[Link](#)]
- Chung, S.-W., S. Jan, and K. K. Liu, 2001: Nutrient fluxes through the Taiwan Strait in Spring and Summer 1999. *J. Oceanogr.*, **57**, 47-53, doi: 10.1023/A:1011122703552. [[Link](#)]
- Dadson, S. J., N. Hovius, H. Chen, W. B. Dade, M. L. Hsieh, S. D. Willett, J. C. Hu, M. J. Horng, M. C. Chen, C. P. Stark, D. Lague, and J. C. Lin, 2003: Links between erosion, runoff variability and seismicity in the Taiwan orogen. *Nature*, **426**, 648-651, doi: 10.1038/nature02150. [[Link](#)]
- Gustafsson, Ö., P. M. Gschwend, and K. O. Buesseler, 1997: Using  $^{234}\text{Th}$  disequilibria to estimate the vertical removal rates of polycyclic aromatic hydrocarbons from the surface ocean. *Mar. Chem.*, **57**, 11-23, doi: 10.1016/S0304-4203(97)00011-X. [[Link](#)]
- Gustafsson, Ö., K. O. Buesseler, W. R. Geyer, S. B. Moran, and P. M. Gschwend, 1998: An assessment of the relative importance of horizontal and vertical transport of particle-reactive chemicals in the coastal ocean. *Cont. Shelf Res.*, **18**, 805-829, doi: 10.1016/S0278-4343(98)00015-6. [[Link](#)]
- Huang, B. Q., H. S. Hong, and H. L. Wang, 1999: Size-fractionated primary productivity and the phytoplankton-bacteria relationship in the Taiwan Strait. *Mar. Ecol. Prog. Ser.*, **183**, 29-38, doi: 10.3354/meps183029. [[Link](#)]
- Hung, C. C., L. D. Guo, K. A. Roberts, and P. H. Santschi, 2004: Upper ocean carbon flux determined by size-fractionated  $^{234}\text{Th}$  data and sediment traps in the Gulf of Mexico. *Geochem. J.*, **38**, 601-611.
- Hung, J. J., P. L. Lin, and K. K. Liu, 2000: Dissolved and particulate organic carbon in the southern East China Sea. *Cont. Shelf Res.*, **20**, 545-569, doi: 10.1016/S0278-4343(99)00085-0. [[Link](#)]
- Hung, J. J., C. H. Chen, G. C. Gong, D. D. Sheu, and F. K. Shiah, 2003: Distributions, stoichiometric patterns and cross-shelf exports of dissolved organic matter in the East China Sea. *Deep-Sea Res. II*, **50**, 1127-1145, doi: 10.1016/S0967-0645(03)00014-6. [[Link](#)]

- Jan, S. and S. Y. Chao, 2003: Seasonal variation of volume transport in the major inflow region of the Taiwan Strait: The Penghu Channel. *Deep-Sea Res. II*, **50**, 1117-1126, doi: 10.1016/S0967-0645(03)00013-4. [[Link](#)]
- Kao, S. J., F. K. Shiah, C. H. Wang, and K. K. Liu, 2006: Efficient trapping of organic carbon in sediments on the continental margin with high fluvial sediment input off southwestern Taiwan. *Cont. Shelf Res.*, **26**, 2520-2537, doi: 10.1016/j.csr.2006.07.030. [[Link](#)]
- Ku, T. L., K. G. Knauss, and G. G. Mathiew, 1977: Uranium in open ocean: Concentration and isotopic composition. *Deep-Sea Res.*, **24**, 1005-1017, doi: 10.1016/0146-6291(77)90571-9. [[Link](#)]
- Liang, W. D., T. Y. Tang, Y. J. Yang, M. T. Ko, and W. S. Chuang, 2003: Upper-ocean currents around Taiwan. *Deep-Sea Res. II*, **50**, 1085-1105, doi: 10.1016/S0967-0645(03)00011-0. [[Link](#)]
- Murray, J. W., J. Young, J. Newton, J. Dunne, T. Chapin, B. Paul, and J. J. McCarthy, 1996: Export flux of particulate organic carbon from the central equatorial Pacific determined using a combined drifting trap-<sup>234</sup>Th approach. *Deep-Sea Res. II*, **43**, 1095-1132, doi: 10.1016/0967-0645(96)00036-7. [[Link](#)]
- Radakovitch, O., M. Frignani, S. Giuliani, and R. Montanari, 2003: Temporal variations of dissolved and particulate <sup>234</sup>Th at a coastal station of the northern Adriatic Sea. *Estuar. Coast. Shelf Sci.*, **58**, 813-824, doi: 10.1016/S0272-7714(03)00187-2. [[Link](#)]
- Santschi, P. H., Y. H. Li, and J. Bell, 1979: Natural radionuclides in the water of Narragansett Bay. *Earth Planet. Sci. Lett.*, **45**, 201-213, doi: 10.1016/0012-821X(79)90121-3. [[Link](#)]
- Santschi, P. H., C. C. Hung, G. Schultz, N. Alvarado-Quiroz, L. Guo, J. Pinckney, and I. Walsh, 2003: Control of acid polysaccharide production and <sup>234</sup>Th and POC export fluxes by marine organisms. *Geophys. Res. Lett.*, **30**, 1144, doi: 10.1029/2002GL016046. [[Link](#)]
- Tung, C. H., 2007: Pigments distribution in coastal surface waters off Taiwan. Master Thesis, National Taiwan University, Taipei, Taiwan, ROC, 65 pp.
- Wei, C. L. and C. C. Hung, 1992: Spatial variation of <sup>234</sup>Th scavenging in the surface water of the Bashi Channel and the Luzon Strait. *J. Oceanogr.*, **48**, 427-437, doi: 10.1007/BF02234019. [[Link](#)]
- Wei, C. L., J. R. Tsai, L. S. Wen, S. C. Pai, and J. H. Tai, 2009: Nearshore scavenging phenomenon elucidated by <sup>234</sup>Th/<sup>238</sup>U disequilibrium in the coastal waters off western Taiwan. *J. Oceanogr.*, **65**, 137-150, doi: 10.1007/s10872-009-0014-z. [[Link](#)]
- Weinstein, S. E. and S. B. Moran, 2005: Vertical flux of particulate Al, Fe, Pb, and Ba from the upper ocean estimated from <sup>234</sup>Th/<sup>238</sup>U disequilibria. *Deep-Sea Res. I*, **52**, 1477-1488, doi: 10.1016/j.dsr.2005.03.008. [[Link](#)]
- Zaneveld, J. R. V., 1994: Optical closure: from theory to measurement. In: Spinrad, R. W., K. L. Carder, and M. J. Perry (Eds.), *Ocean Optics*. Oxford Monographs on Geology and Geophysics, No. 25. Oxford University Press, Oxford, 59-72.